Modelling of Wind Turbines as Porous Disks for Wind Farm Flow Studies

Journal of Physics: Conference Series **2767** (2024) 052049 doi:10.1088/1742-6596/2767/5/052049

Modelling of Wind Turbines as Porous Disks for Wind Farm Flow Studies

M. Catania, G. Pomaranzi, A. Fontanella and A. Zasso

Dept. of Mechanical Engineering, Politecnico di Milano, via La Masa 1, 20156 Milano, Italy

E-mail: giulia.pomaranzi@polimi.it

Abstract. This study explores the use of porous disks as a modeling approach for wind turbines in both wind tunnel experiments and computational fluid dynamics (CFD) simulations. Experimental testing is conducted on a 0.2m diameter disk made of wired mesh, measuring its wake for several yaw angles. The experiment is recreated in a CFD environment based on the porous-medium approach. The CFD model is validated against part of the measurements and it is used to further investigate the disk wake. Results indicate the porous disk wake resembles that of a wind turbine, especially at a downstream distance of four diameters, and the CFD model effectively captures the disk behavior. Discrepancies between experiment and CFD appear further downstream mainly due to the wake recovery process being only partially captured by the CFD model. When the disk has a yaw angle the wake is displaced laterally, but less than in a widely-accepted deflection model, and this could be due to the lack of wake curling.

1. Introduction

Wind turbines are often installed in large clusters, where the relatively short distance between units makes individual machines interact through their wakes. Wake interactions typically occurring in wind farms negatively affect power production and wind turbine loads, thus they should be carefully modeled when designing wind plants. In this context, wind tunnel experiments provide valuable information about the physics of wakes and support their theoretical modeling [1]. When modeling is focused on the inflow inside the farm rather than the response of individual turbines, it is convenient to rely on a macroscopic representation of the interaction between atmospheric wind, wakes, and rotors. Within a computational fluid dynamics (CFD) framework, this is usually achieved through the actuator disk approach which represents the rotor as a circular region where a momentum deficit is created. The actuator disk is realized in the wind tunnel environment with a disk of porous material [2, 3].

The actuator disk approach and its physical representation have been used in a number of studies about wakes. In [4] the actuator disk model is leveraged in a large-eddy simulation to understand how the wake center trajectory changes with a rotor-yaw angle. Wind tunnel experiments with porous disks are conducted in [5, 6] to measure the wake deflection with static and dynamic yaw. In [3], nine research teams organized a round-robin experiment on porous disks in an attempt to rationalize their use to mimic the wake of wind turbines. Recently, a porous-disk rotor model has been used to investigate the wake response to platform motion in floating wind turbines [7].

The main objective of this work is to investigate the use of porous disks to reproduce wind turbines and their wake. In particular, we test the possibility of using the disk to reproduce the wake lateral deflection, which is one of the most widely used wind farm flow control methods. To this purpose we carry out wind tunnel experiments and we introduce a CFD model which mimics the physics of the interaction between disk and flow. The CFD model is validated against wind tunnel measurements and then used to extend the study of the flow over the full wind tunnel domain, where measurements are not available, thus gaining a deeper understanding of the porous disk wake generation mechanisms.

The experimental results and computational methods developed in this work add to previous research on porous disks. This should help move towards more shared practices on how to use the porous disk technology in a wind tunnel and in numerical simulations, in particular for wake flow interaction and control studies.

The article is organized in this way. Section 2 describes the modeling of the porous disk in the wind tunnel experiment and in the CFD framework. Section 3 presents the results of the experiment, of the validation of the CFD model versus wind tunnel data and explores the wake deflection in the porous disk comparing measurements and CFD results to an analytical wake deflection model. Results are discussed in Sect. 4 before drawing the conclusions in Sect. 5.

2. Methodology

The feasibility of employing a porous disk as a wake-generating device is tested in a wind tunnel experiment monitoring the velocity deficit evolution in the far wake region. The disk is tested in various yaw angles (θ), specifically at $\theta = [0°, 10°, 20°, 30°]$ to simulate wake steering control. Subsequently, the experimental test is replicated within the CFD environment. Departing from the conventional actuator disk model, which necessitates approximations of disk velocity and thrust force distribution (e.g., through indicator functions [8]), the porous disk is modeled using a porous-medium approach. This modelling strategy closely mimics the physics of the porous material, but does not require to introduce in the computational domain the porous element geometry, since it provides a macroscopic description of the flow interaction with the porous disk. The porous-medium modeling technique has been employed in several fields, for example for the simulation of ventilation systems [9] and to study the interaction between wind and buildings facades [10]. The CFD model is validated against wind tunnel data and, after that, it is used to study the wake deflection and deformation.

In wind farm flow studies it is fundamental to capture the lateral wake deflection due to a rotor misalignment since this principle is often leveraged for wind farm control. To verify the consistency of the wake lateral displacement due to yaw obtained with the porous disk approach, experimental and CFD results are compared with a recognized wake deflection model.

2.1. Experimental testing

A 0.2 m diameter (D) porous disk (Fig. 1), is tested in the high-speed section of Politecnico di Milano wind tunnel in steady-uniform and smooth flow ($U = 5.5\ m/s$ and $I_u = 0.2\%$). The test section has dimensions of 4 m wide, 4 m high, 4 m long. Velocity measurements are carried out with a one-component hot-wire anemometer at hub height at distances of $x = 4D$ and $x = 8D$ from the disk to characterize the wake. Measurements span a line in the cross-stream direction of $\pm 1.5\ D$, with $0.1\,D$ resolution. The porous disk is made of a wired mesh with a porosity of 43%, defined as the ratio between the empty and total surfaces. Uncertainty in velocity experimental acquisitions is mainly due to possible misalignment in hot wire positioning: errors in the identification of the wake center are estimated to be in the order of the measurement resolution.

The fluid-dynamic characteristics of the porous material are characterized through the pressure-loss coefficient k, defined as the pressure drop between the upwind and downwind

sides of the porous element normalized by the dynamic pressure. k is evaluated experimentally with dedicated testing in an open circuit wind tunnel with a circular cross-section of 0.4 m diameter; the inflow is approximately laminar.

(a) (b)

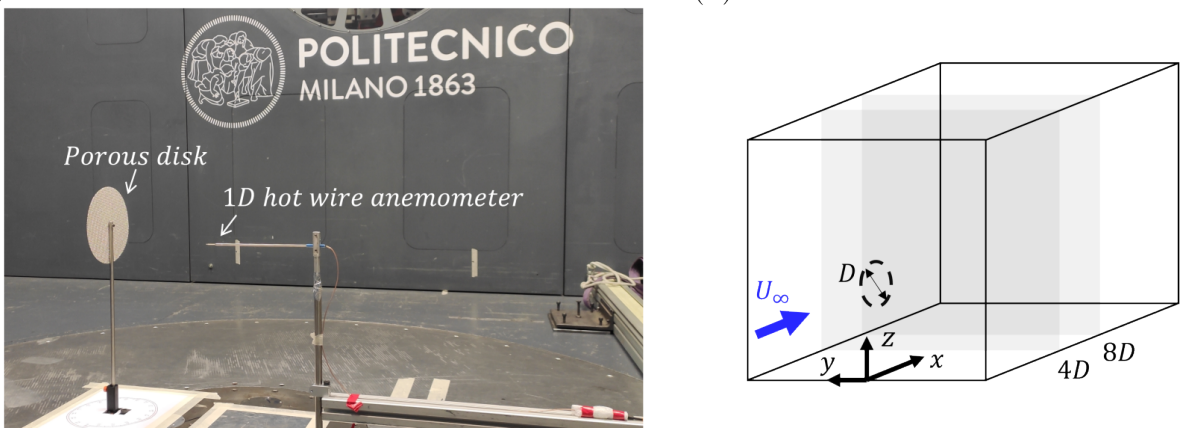

Figure 1. Wind tunnel setup. **(a)** The porous disk inside the wind tunnel test section with the hot-wire anemometer. **(b)** Coordinate system and position of the wake measurement planes.

2.2. CFD model

A CFD study is carried out to extend the experimental results and to gain a deeper understanding of the wake-generation mechanism of the porous disk. Within a CFD framework, one of the most efficient ways to represent a porous object is to rely on a macroscopic representation through a porous-medium approach, avoiding an explicit modeling of the porous layer geometry. In the porous-disk CFD model, the disk is represented as a volume where a sink term $\mathbf{s} = [s_x, s_y, s_z]'$ is added to the momentum balance equation. According to the Darcy-Forchheimer law, the sink term is defined as:

$$\mathbf{s} = -\mu \mathbf{D}\mathbf{u} - \frac{1}{2}\rho U \mathbf{F}\mathbf{u}\,, \tag{1}$$

where $\mathbf{u} = [u_x, u_y, u_z]'$ is a vector of the fluid velocity components, $U = \|\mathbf{u}\|$, μ and ρ are the air viscosity and density, $\mathbf{D}$ and $\mathbf{F}$ are the Darcy and Forchheimer tensors respectively. In this case, $\mathbf{D}$ and $\mathbf{F}$ are diagonal matrices.

In the current study, the porous disk is made of wired mesh, thus the viscous stresses expressed by the first term of Eq. 1 can be neglected. This is because the flow interaction with the porous disk is expected to be dominated by pressure forces rather than the fluid viscous forces [10]. Then, assuming an incompressible steady-state flow, the momentum balance equation at the root of the CFD model becomes:

$$u_j \frac{\partial u_i}{\partial x_j} = \frac{1}{\rho}\frac{\partial p}{\partial x_i} - \frac{1}{2} U f_i u_i \quad \text{with } i, j = x, y, z\,, \tag{2}$$

where p is the fluid pressure, f_i are the terms of $\mathbf{F} = \mathrm{diag}(f_x, f_y, f_z)$ and they represent the resistance of the wired mesh forming the disk. In addition, considering the rotational symmetry of the wire mesh, we have $f_y = f_z$.

2.2.1. Characterisation of the resistance coefficients. The coefficient f_x, which characterizes the resistance term when the flow is normal to the disk, can be determined by dividing the measured pressure-loss coefficient k by the thickness of the porous volume in the computational domain h. While the resistance terms in other directions are not directly measured experimentally, they are computed using the methodology proposed by [10], which compares the forces experienced by the porous element with explicit modeling versus those derived from the porous-medium approach. This approach leads to $f_y = f_z \simeq 0.5 f_x$. A similar relationship among f_x, f_y and f_z has been proposed by [11], who performed high-fidelity CFD simulations on porous elements that satisfy the same symmetry conditions as the wire mesh considered in this study. Furthermore, a sensibility analysis conducted on the tensor's coefficients highlights that the most accurate representation of the wake behind a wired mesh disk is achieved with the proposed tensor. Higher values of the coefficients in the y and z directions tend to alter the velocity profile and overestimate the wake lateral displacement in presence of a yaw angle. Hence the resistance term adopted in Eq. 2 is:

$$\mathbf{F} = \frac{1}{h}\begin{bmatrix} 1.60 & 0 & 0 \\ 0 & 0.75 & 0 \\ 0 & 0 & 0.75 \end{bmatrix}.$$

2.2.2. Numerical Setup. The computational domain mimics the experimental environment, as depicted in Fig. 2. The domain is symmetric with respect to the vertical plane passing through the disk and has wall-boundary conditions to represent the wind tunnel walls. The region of the wind tunnel occupied by the porous disk is replaced in the simulation by a porous volume. The thickness of the porous volume is $h = 0.05$ m; the mesh has been refined in correspondence of the porous volume to have at least 5 cells in the x direction. This is required to properly realize the momentum deficit $\mathbf{s}$ of Eq. 1.

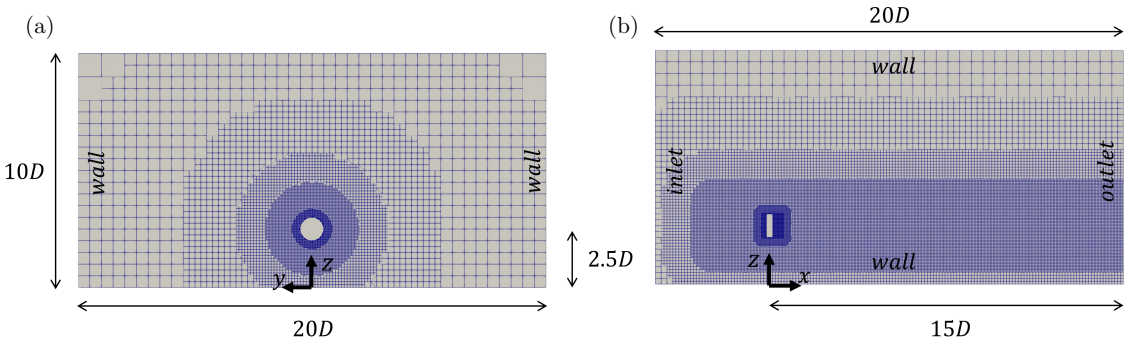

Figure 2. Computational domain. **(a)** front view. **(b)** side view.

The numerical simulations are performed using a steady-state Reynolds-Averaged Navier-Stokes (RANS) solver and a second-order differentiation scheme. The $k-\epsilon$ model has been used because, in a preliminary investigation on the case, it proved to be more accurate than the $k-\omega$ Shear Stress Transport (SST) in predicting the wake characteristics. The computational domain is meshed with 1.5 million hexahedral elements and five refinement levels. The independence of the results on the mesh refinement has been checked and is not reported here for brevity.

2.3. Analytical model of the wake deflection

A simple analytical method to calculate the wake deflection due to a rotor misalignment is the equation proposed by Jimenez [4], which is derived based on axial-momentum conservation.

According to this model, the lateral displacement of the wake center (y_c) is:

$$\frac{y_c}{D} = \cos\theta^2 \sin\theta \frac{C_T}{2} \frac{1}{\beta} \left(1 - \frac{1}{\beta x/D + 1}\right) , \tag{3}$$

where θ is the angle between the rotor axis and the incoming flow (i.e., the yaw angle in this case), C_T is the thrust coefficient, and β is the wake-width growth rate. In our calculations $C_T = 0.65$. C_T has been computed from the integral of the momentum deficit of wakes measured in the wind tunnel experiment with $\theta = 0°$ and confirmed by the CFD model, where it is evaluated as the integral of pressure forces over the disk with zero yaw angle. β has been set equal to 0.1, that is in the range of typical values suggested in [4].

2.4. Limitations of the porous disk approach with respect to wake swirl

Blades of a wind turbine rotor generate forces in the rotor plane that are not emulated with the porous disk approach. The in-plane forces are associated with rotational momentum and wake swirl. Previous research has shown the transversal velocity due to rotor in-plane forces becomes insignificant after 3D because the rotational flow is dissipated by turbulent diffusion [2].

In presence of a yaw misalignment, the wake swirl introduces additional asymmetry of the far-wake shape that is neglected with the porous disk approach, in both the experiment and its CFD model. However, the contribution of swirl on wake deflection is small compared to other effects [12] and it is fair to neglect it in first approximation.

3. Results

Section 3.1 reports results of the aerodynamic characterization of the porous mesh forming the disk. In Sect. 3.2 we present the results of the wind tunnel experiment, in Sect. 3.3 we show results of the CFD model and we compare them to measurements in order to validate our calculations. Subsequently, in Sect. 3.4 we study the wake deflection of the porous disk and we compare experimental and CFD results to the analytical model of Sect. 2.3.

3.1. Aerodynamic characteristics of the wire mesh

The pressure loss coefficient k is measured experimentally with the methodology discussed in Sect. 2.2.1 varying the inlet velocity between 3 and 10 m/s. It has been found that in this velocity range $k = 1.65$ with a variability of $\pm 1.5\%$. Thus, k can be then considered as Reynolds independent within the tested velocity range and the tensor $\mathbf{F}$ coefficients for the CFD model are here assumed not varying with Reynolds.

3.2. Wind tunnel results

Figure 3 shows the wake velocity normalized with respect to the free-stream wind speed U_∞ at $x = [4D, 8D]$ for various yaw angles. At a distance of $x/D = 4$, the wake exhibits a flatter profile compared to a bladed rotor, while at $8D$, it demonstrates a Gaussian shape. The minimum velocity is obtained with a yaw angle of $\theta = 0°$, reaching 45% of the undisturbed velocity U_∞, consistently with previous investigations on the same porous disk by [3]. Application of a yaw angle results in a lateral movement of the wake center, as expected from theory.

3.3. CFD results

The CFD porous-medium approach provides a set of results comparable to those obtained in the experiment. Wake velocity profiles are extracted at $4D$ and $8D$ downstream the disk and compared in Fig. 4 to those of the experiment for yaw angles of $\theta = 0°$ and $30°$. At $x/D = 4$, the CFD closely aligns to wind tunnel measurements in terms of velocity deficit, wake shape and wake deflection. At $x = 8D$, the CFD model captures accurately the shape of the velocity

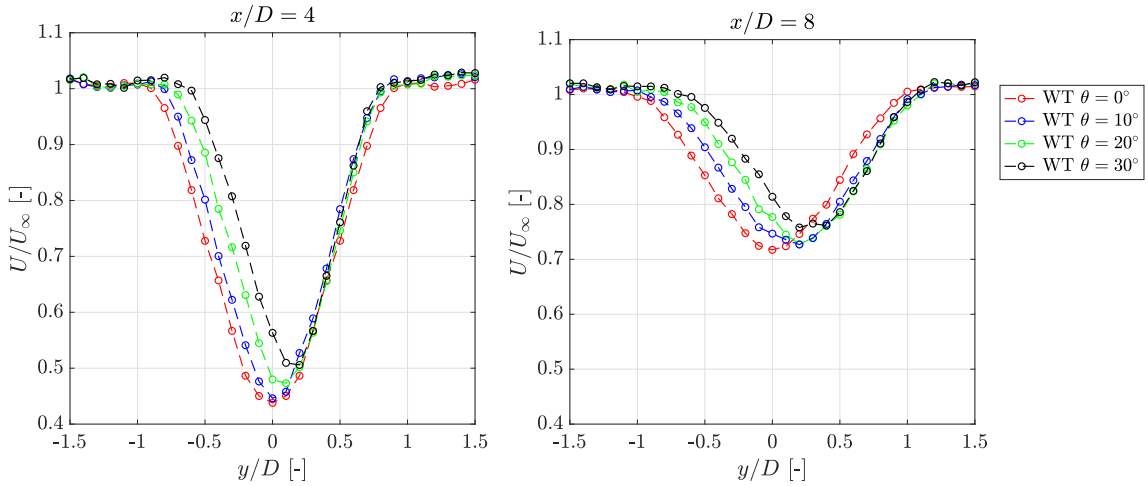

Figure 3. Normalized wind speed in the disk wake at $x/D = 4$ and $x/D = 8$ from wind tunnel measurements (WT).

profile of experimental data, although it predicts a weaker recovery of the wake, underestimating the minimum velocity by 15% for $\theta = 0°$.

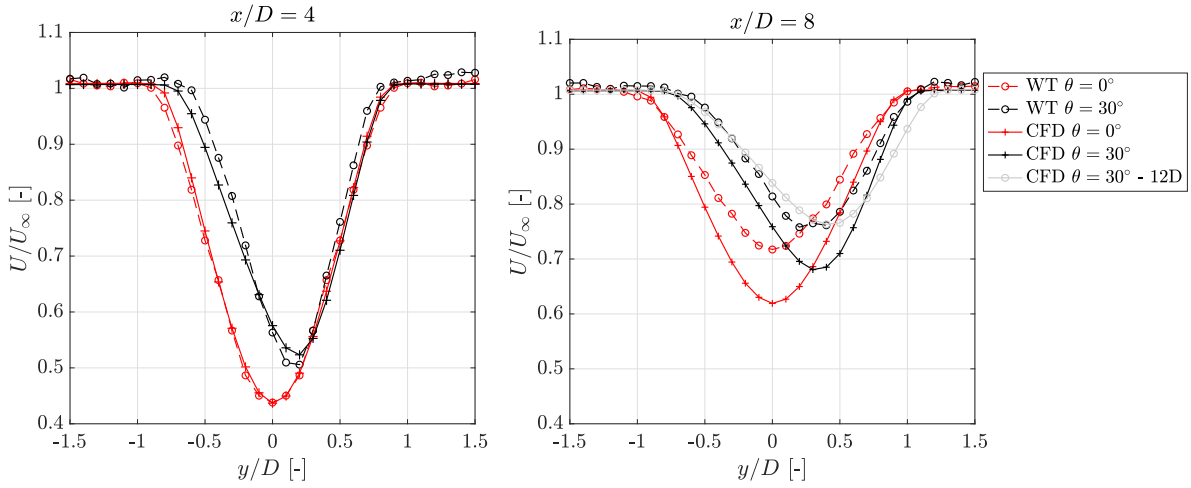

Figure 4. Normalized axial wind speed in the disk wake at $x/D = 4$ and $x/D = 8$ from wind tunnel measurements (WT) and the CFD model.

Comparing the experimentally-measured wake with the CFD results, it can be observed that the experimental wake profile at $8D$ aligns with the corresponding CFD at $12D$ downstream. The under-prediction of the recovery rate from the CFD is consistent with prior studies about the performances of RANS simulations of actuator disks [13], which noted some limitations of the standard $k - \epsilon$ turbulence model when modeling the wake behavior.

Figure 5 shows the wake velocity predicted by the CFD model on vertical planes at $4D$, $8D$, and $12D$ downstream the disk location. With $\theta = 0°$ the wake shape is symmetric with respect to the disk axis. Instead, with $\theta = 30°$ the wake is shifted laterally and is slightly asymmetric.

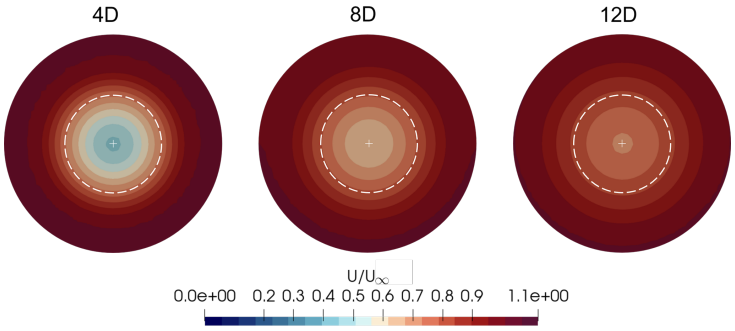

(a) $\theta = 0°$.

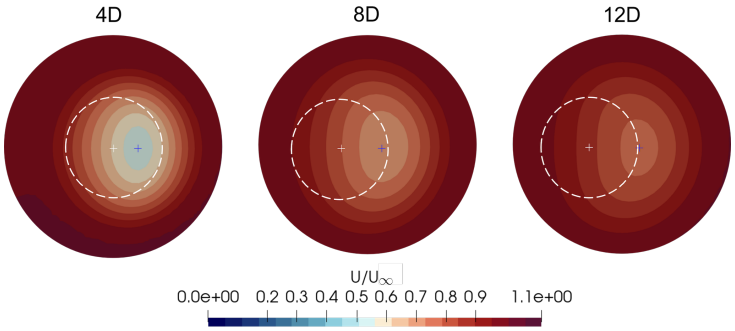

(b) $\theta = 30°$.

Figure 5. Normalized velocity contour plot (U/U_∞) at different sections along the wake (x/D) obtained from the CFD study. The disk edge is marked by a dashed white line, the wake center with a blue cross.

3.4. Lateral wake deflection due to yaw

We studied the wake deflection at several distances downstream the disk. The wake deflection is computed as the lateral displacement of the wake center from the centerline (i.e., y_c).

Figure 6 compares values of y_c obtained in the experiment and in the CFD model to the Jimenez model of Eq. 3 for yaw angles of 10°, 20°, and 30°. Experimental data are represented by markers at $4D$ and $8D$ and the error bars show their uncertainty.

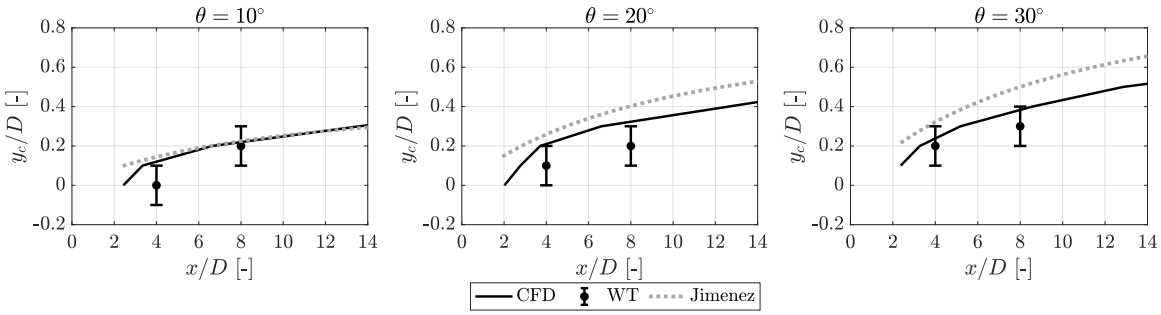

Figure 6. Non-dimensional wake centerline position (y_c/D) along the axial direction (x/D) and at hub height, for three values of the disk yaw angle θ. y_c is obtained from the CFD model, wind tunnel measurements (WT) and the Jimenez model [4]. Error bars of experimental results show the uncertainty of y_c related to the measurement procedure.

The CFD model reproduces the wake deflection of the experiment with reasonable accuracy confirming it catches the wake generation process of the porous disk. Deviations between experiment and CFD are equally important at all the yaw angles.

Concerning the comparison with the Jimenez model, simulations and experimental results generally follow the trend of Eq. 3. However, the wake deflection in the porous disk, both in the experiment and CFD, is lower than in the analytical model and the difference increases for higher yaw angles. For $\theta = [20, 30]^\circ$ the wake deflection in the experiment is 19% and 21% lower than in the Jimenez model.

4. Discussion of results

The capability of a porous disk to replicate the wake behavior of a bladed rotor is assessed under different yawed configurations. At $x/D = 4$ the porous disk generates a Gaussian-shaped wake both in the experiment and the CFD model. Considering yawed configurations, the wake center is shifted laterally by a similar amount in the experiment and CFD simulations.

Moving further downwind, at $x/D = 8$, the CFD under-estimates the wake recovery rate, predicting a lower velocity than in the experiment. This is likely due to the RANS approach which is convenient in terms of computational cost, but lacks accuracy in modeling the turbulence production from vortex breakdown that drives the wake recovery [14]. To overcome such limitations, a viable solution could be to include source terms in the transport equation to reflect the contributions of the turbulent kinetic energy. The models proposed in [15, 16, 17] have been tested with a wide set of experimental data and Large-Eddy CFD Simulations (LES), showing different degrees of accuracy. However, it is difficult to generalize the application of these models since a parameter calibration on the experimental case is always required [18, 19].

Moreover, it is expected from previous research (e.g., [5]) that the wake of a yawed wind turbine rotor displays significant spanwise asymmetry, known as curled wake, greater than what is shown in Fig. 5b. The wake deformation is induced by a couple of counter-rotating vortices originating at the top and the bottom of the rotor disk and it has been proven both with an integral representation of rotor loads (i.e., an actuator disk) or considering blade loads. The generation of the counter-rotating vortices seems underestimated in the CFD simulations. This is mainly due to the adopted turbulence model, which underestimates the vorticity induced by the disk in the downstream flow.

Finally, when the disk is misaligned with respect to wind its wake is deflected laterally, and the amount of deflection in the experiment is generally consistent with its CFD model, deviations between experiment and CFD are equally important with all yaw angles that were tested.

The wake deflection obtained in the experiment and in the CFD is up to 20% lower than what is predicted by the Jimenez model, and the difference is proportional to the amount of disk misalignment. Deviations between the lateral wake deflection of a porous disk and predictions of the Jimenez model have also been reported by other studies, e.g., [6]. These differences could be related to the assumptions of the Jimenez model: for example it uses the thrust coefficient of the zero yaw case also when the yaw is different from zero. Nevertheless, the wake trajectory of the porous disk displayed by the CFD, is consistent with the Jimenez model, which is widely used for wake deflection studies. Therefore, we conclude that the porous disk is a suitable approach to reproduce wake deviations due to misalignment.

5. Conclusions

This study investigated the use of porous disks to replicate wind turbine wakes in wind tunnel experiments and CFD simulations.

The experimental setup involves a 0.2 m diameter porous disk tested in a wind tunnel with yaw angles from 0° to 30°. The CFD model employs a porous-medium approach, departing from conventional actuator disk models, to simulate the flow interaction with the porous disk. The

results from wind tunnel experiments and CFD are compared, revealing a good agreement in the wake characteristics at $x = 4\ D$. The CFD model tends to underestimate the wake recovery rate at $x = 8\ D$, highlighting limitations in capturing the wake turbulent production and mixing with the undisturbed wind, which might be solved in future by improving the turbulence model or by artificially increasing the vorticity.

To understand if the porous disk can mimic the wake of a yawed wind turbine rotor, we compared the wake deflection obtained from experiments and CFD with an analytical model proposed by Jimenez. A wake deflection is present and is consistent in the experiment and CFD, but it is slightly less than in the analytical model, especially with the largest yaw angle.

Overall, the porous disk approach is simple and easily implemented in a CFD environment and in wind tunnel experiments. It is effective in reproducing wake deficit and wake lateral displacement and this makes it suitable for studies on farm-wide interactions between atmospheric wind, wakes, and rotors.

References

[1] Meyers J, Bottasso C, Dykes K, Fleming P, Gebraad P, Giebel G, Göçmen T and van Wingerden J W 2022 *Wind Energy Science* **7** 2271–2306 URL https://wes.copernicus.org/articles/7/2271/2022/

[2] Aubrun S, Loyer S, Hancock P and Hayden P 2013 *Journal of Wind Engineering and Industrial Aerodynamics* **120** 1–8 ISSN 0167-6105 URL https://www.sciencedirect.com/science/article/pii/S0167610513001220

[3] Aubrun S, Bastankhah M, Cal R, Conan B, Hearst R, Hoek D, Hölling M, Huang M, Hur C, Karlsen B, Neunaber I, Obligado M, Peinke J, Percin M, Saetran L, Schito P, Schliffke B, Sims-Williams D, Uzol O, Vinnes M and Zasso A 2019 *Journal of Physics: Conference Series* **1256** 012004 URL https://dx.doi.org/10.1088/1742-6596/1256/1/012004

[4] Jiménez Crespo A and Migoya E 2010 *Wind Energy* **13** 559–572 (*Preprint* https://onlinelibrary.wiley.com/doi/pdf/10.1002/we.380) URL https://onlinelibrary.wiley.com/doi/abs/10.1002/we.380

[5] Howland M F, Bossuyt J, Martínez-Tossas L A, Meyers J and Meneveau C 2016 *Journal of Renewable and Sustainable Energy* **8** 043301 ISSN 1941-7012 (*Preprint* https://pubs.aip.org/aip/jrse/article-pdf/doi/10.1063/1.4955091/13852526/043301_1_online.pdf) URL https://doi.org/10.1063/1.4955091

[6] Macrì S, Coupiac O, Girard N, Leroy A and Aubrun S 2018 *Journal of Physics: Conference Series* **1037** 072035 URL https://dx.doi.org/10.1088/1742-6596/1037/7/072035

[7] Schliffke B, Aubrun S and Conan B 2020 *Journal of Physics: Conference Series* **1618** 062015 URL https://dx.doi.org/10.1088/1742-6596/1618/6/062015

[8] Heck K, Johlas H and Howland M 2023 *Journal of Fluid Mechanics* **959** A9

[9] Packwood A 2000 *Journal of Wind Engineering and Industrial Aerodynamics* **88** 75–90 ISSN 0167-6105 URL https://www.sciencedirect.com/science/article/pii/S0167610500000258

[10] Pomaranzi G, Bistoni O, Schito P and Zasso A 2021 *Wind and Structures* **33** 409–422 URL https://doi.org/10.12989/was.2021.33.5.409

[11] Chen H and Christensen E D 2016 *Journal of Fluids and Structures* **65** 76–107

[12] van den Broek M J, De Tavernier D, Hulsman P, van der Hoek D, Sanderse B and van Wingerden J W 2023 *Wind Energy Science* **8** 1909–1925 URL https://wes.copernicus.org/articles/8/1909/2023/

[13] MacLeod A, Barnes S, Rados K and Bryden I 2002 Wake effects in tidal current turbine farms *International conference on marine renewable energy-conference proceedings* pp 49–53

[14] Batten W M J H M E and S B A 2013 *Philosophical transactions of the Royal Society A* **371** URL http://doi.org/10.1098/rsta.2012.0293

[15] Crespo A, Manuel F, Moreno D, Fraga E and Hernandez J 1985 Numerical analysis of wind turbine wakes *Workshop on Wind Energy Applications, Delphi, Greece* pp 15–25

[16] Cabezón Martínez D, Sanz Rodrigo J, Martí Pérez I and Crespo Martínez A 2009

[17] Van Der Laan M P, Sørensen N N, Réthoré P E, Mann J, Kelly M C, Troldborg N, Schepers J G and Machefaux E 2015 *Wind Energy* **18** 889–907

[18] Réthoré P E 2009 Wind turbine wake in atmospheric turbulence URL https://api.semanticscholar.org/CorpusID:120286021

[19] Prospathopoulos J M, Politis E S, Rados K G and Chaviaropoulos P K 2011 *Wind Energy* **14** 285–300 URL https://api.semanticscholar.org/CorpusID:110665411